

1 Bedrock type mediates the response of vegetation growth to seasonal
2 precipitation in the karst zone of subtropical China

3

4 **Zihan Jiang¹, Hongyan Liu^{1,*}, Xu Liu¹, Jingyu Dai¹, Xiuchen Wu², Jian Peng¹, Hongya
5 Wang¹, Jeroen Meersmans³, Sophie M. Green⁴, Timothy A. Quine⁴**

6

7 *1. College of Urban and Environmental Sciences and MOE Laboratory for Earth Surface*

8 *Processes, Peking University, Beijing, 100871, P.R. China;*

9 *2. Faculty of Geographical Sciences, Beijing Normal University, Beijing, 100875, P.R. China;*

10 *3. Cranfield Soil and Agrifood Institute, School of Water, Energy and Environment, Cranfield*

11 *University, Cranfield, MK43 0AL, United Kingdom*

12 *4. Geography, CLES, University of Exeter, Exeter, EX4 4SB, United Kingdom*

13

14

15 * Corresponding author (email: lhy@urban.pku.edu.cn)

16

17

18

19 **Abstract:** Low water conservation ability of carbonate limits vegetation growth in karst landscape has
20 been commonly recognized, but how bedrock mediates the effect of precipitation on vegetation growth
21 remains unclear. We studied the spatio-temporal differences of vegetation growth in Guizhou Province
22 of China by dividing the study region into three types of lithological region based on stream sediment
23 geochemical data. The differences of precipitation-vegetation growth relationship among them were
24 assessed. The results show that in months with low precipitation (0–150 mm), lower vegetation growth
25 occurs in regions where the bedrock has higher calcium (Ca) content, whereas in months with high
26 precipitation (150–250 mm), significant differences are not observed in the vegetation growth among
27 various lithological regions. Extremely high amount of precipitation (>250 mm) can even benefit
28 vegetation growth on the karst landscape. Our findings highlight that there is a threshold of
29 precipitation amount for limiting vegetation growth in the karst landscape, which should be taken into
30 account when studying responses of vegetation growth to climate change in the karst landscape.

31

32 **Keywords:** carbonate rock, karst, intermittent drought, enhanced vegetation index, temporal and spatial
33 distribution of precipitation

34

35 **1. Introduction**

36 Restricted vegetation growth in karst region has been commonly attributed to the low water
37 conservation ability of the regolith (Hamp et al., 2014; Morford et al., 2011; Neff et al., 2006; Wang et
38 al., 2010), although surface climate and soil conditions have been considered the main cause of the
39 spatial variations in vegetation growth (Fridley et al., 2011; Guay et al., 2014; Lobell et al., 2015;
40 Medlyn et al., 2016). Despite the recognition of bedrock on vegetation growth, how bedrock mediates
41 the effect of precipitation on regional vegetation growth, however, remains unclear.

42 The main challenges of evaluating the mediation of bedrock lie on spatial heterogeneity of
43 bedrock distribution and the high costs involved in quantifying chemical and physical constituents of
44 bedrock samples, which limits high-precision rock sampling within large areas. Stream sediments are
45 products of re-precipitation after rock weathering; such sediments are mechanically transported by or
46 dissolved in and then transported by surface runoff or groundwater into stream systems (Cheng and
47 Agterberg, 2009). Extensive research demonstrates that the contents of stream sediments are close to
48 the average element contents of rocks in the upstream catchment basin (Albanese et al., 2007; Vital and
49 Stattegger, 2000). Recent research has found significant chemical element similarities between stream
50 sediments and rocks on a large scale, which provides an excellent tool for analysing the effects of
51 bedrock-mediated available water on vegetation (Kirkwood et al., 2016).

52 Vegetation in carbonate zones might be easily affected by drought during low precipitation
53 seasons, whereas vegetation in non-carbonate zones can use water contained in deep soil layers during
54 drought episodes, thus have greater resilience to drought episodes. Under sufficient precipitation, the
55 difference in vegetation productivity between carbonate and non-carbonate zones is expected to
56 disappear. In this study, we hypothesized that vegetation growth patterns differed among bedrock types.
57 In other words, vegetation growth is slower in carbonate zones during periods with lower precipitation
58 than in non-carbonate zones; as precipitation increases, such differences may not exist.

59 Regions underlain by carbonate rocks in Guizhou Province situated in subtropical China account
60 for 66% of its total area. A relatively large variety of lithological types with complex compositions
61 occurs in Guizhou. In addition, karst landforms have developed in most regions. Due to their low water
62 conservation ability, karst ecosystems are extremely vulnerable and prone to rocky desertification
63 characterized by reduced vegetation cover and severe erosion of soil (Zhan et al., 2013). Field
64 observations have found that regions with high rock CaCO_3 content in Guizhou have developed large

65 numbers of cracks and undergone more significant rocky desertification (Sun et al., 2002). However,
66 how lithology is linked to drought that affects vegetation growth remains unclear. The main objective
67 of this study is to investigate the indirect effects of lithology–associated drought that affect vegetation
68 growth in Guizhou Province based on remote sensing, climate and stream sediment data, and to answer
69 the following two questions:

70 (1) Does lithology affect vegetation growth by regulating the relationship between precipitation
71 and vegetation?

72 (2) Is vegetation growth more sensitive to droughts in regions with more carbonate rocks and
73 more severe soil erosions?

74

75 2. Study area

76 Situated in subtropical China (24°30'–29°13'N, 103°1'–109°30'E), Guizhou Province encompasses
77 an area of 176,167 km², of which 66% has carbonate bedrock and the remaining approximately 34%
78 (mainly distributed in the south, southwest and north) has clastic and igneous rock substrates. The
79 study area has a subtropical humid monsoon climate with annual average temperatures of 11–20 °C and
80 annual precipitation of 730–2,300 mm. Significant seasonal changes in precipitation occur, and 75% of
81 the annual precipitation occurs in summer and fall (June–October, based on meteorological station data
82 statistics for the period 2001–2010).

83

84 3. Data sources and methods

85 The precipitation data used in this study originated from monthly data collected at 78
86 meteorological stations for the period 2001–2010 and downloaded from the National Meteorological
87 Information Center of China (<http://data.cma.cn/user/toLogin.html>). The enhanced vegetation index
88 (EVI) can reflect the growth conditions of vegetation and is often used to monitor vegetation growth.
89 The EVI data used in this study originated from Moderate Resolution Imaging Spectroradiometer
90 (MODIS) sensor data (resolution: 500 m; time interval: 16 days)
91 (<https://ladsweb.modaps.eosdis.nasa.gov/>) for the period 2001–2010.

92 The geochemical distribution data for stream sediments used in this study originated from the
93 *Geochemical Atlas of Guizhou Province* (Feng, 2009). This atlas was prepared using loaded regional
94 geochemical survey data for Guizhou Province at a 1:200,000 scale. The whole Guizhou Province was

95 divided into 1 km² sampling units. At least one sampling point was set in each sampling unit, mainly in
 96 the middle of secondary stream systems and at the mouths of primary stream systems. A total of
 97 464,004 stream sediment or diluvial soil samples were collected. During the atlas preparation process,
 98 the concentrations of each chemical element were divided into 12 levels statistically.

99

100 3.2 Data analysis

101 The monthly precipitation recorded at the meteorological stations was interpolated using the
 102 kriging interpolation method. Precipitation in regions with various levels of calcium (Ca) concentration
 103 was calculated using regional analysis. Thus, precipitation time-series data was obtained. The EVI data
 104 was corrected, and unclear images removed. The EVI for each month was calculated. Similarly,
 105 precipitation time-series data for regions with various levels of Ca concentration were also calculated
 106 by regional analysis.

107 Because the extent and erosion rate of carbonate rocks are determined by the fractions of calcite
 108 and dolomite, geochemical differences in Ca can reflect the differences in bedrock. To simplify the
 109 analysis, the EVI time-series data for different regions were subjected to cluster analysis. Because the
 110 complexity of time series affects the estimate of the difference between separate time series, a
 111 complexity-invariant dissimilarity (CID) measure (see equation below) was used to calculate the
 112 distance between any two EVI time series (Serrà and Arcos, 2014).

113

$$114 \quad CE(X_T) = \sqrt{\sum_{t=1}^{T-1} (X_t - X_{t+1})^2}$$

$$115 \quad CF(X_T, Y_T) = \frac{\max\{CE(X_T), CE(Y_T)\}}{\min\{CE(X_T), CE(Y_T)\}}$$

$$116 \quad d_{CID}(X_T, Y_T) = CF(X_T, Y_T) \cdot d(X_T, Y_T)$$

117 where X_T and Y_T represent time series X and Y , respectively; $CE(X_T)$ is the variability of time
 118 series X ; $CF(X_T, Y_T)$ is a complexity correction factor; and $d_{CID}(X_T, Y_T)$ is the distance between time
 119 series X and Y .

120 To analyse the differences in the EVI between rocks with various levels of Ca in different months,
 121 a multi-sample t -test was performed (Cressie and Whitford, 2010). Prior to the t -test, the normal

122 distribution of each set of data was determined. Data that failed to conform to a normal distribution
123 were transformed using log-transformation. Calculations involving the EVI were performed using
124 ArcGIS. The *t*-test and cluster and discriminant analysis were conducted using the "TSdist" package for
125 the R statistical software (Mori et al., 2016).

126

127 **4. Results**

128 **4.1 Division of lithological regions and their characteristics of plant growth**

129 Based on the calculation results for the CID measure, grids with 12 levels of Ca content were
130 clustered into three types (Fig. 1): I. regions with stream sediments having Ca contents lower than
131 25.6%; II. regions with stream sediments having Ca contents greater than 25.6% but lower than 50.7%;
132 and III. the remaining regions with a Ca content greater than 50.7%. A clustering score of 8.65 (full
133 score: 10) indicates that the discriminant analysis based on the CID measure reflects the difference
134 between clusters relatively well.

135 The clustering results were validated using the lithology distribution map. The results show that
136 100% of the Type I regions contain clastic and igneous rocks with no rocky desertification (vegetation
137 degradation in the karst region), that 85% of the Type II regions contain limestone or dolomite (of
138 which 65% have undergone rocky desertification), and that 90% of the Type III regions contain
139 limestone (of which 25% have undergone severe rocky desertification). These validation results
140 demonstrate that geochemical distribution data for stream sediments can satisfactorily reflect the
141 difference in bedrock and soil erosion situations.

142 The temporal change of EVI among three lithological regions were similar (Fig. 2): all of three
143 lithological regions show lower EVI in spring (Jan-Mar) and winter (Oct-Dec), and the peak exhibit in
144 Aug. The EVI of type I lithological region significantly higher than type II and III in each month, but
145 the difference change across time, the greatest difference of EVI among three lithological zone were
146 more pronounced in spring and winter, whereas the differences were lower during summer (Jun-Aug).

147

148 **4.2 Characteristics of precipitation in different lithological regions**

149 Precipitation in Guizhou exhibits relatively significant temporal heterogeneity (Fig. 3). The
150 statistical precipitation data for the period 2001–2010 show that 61% of the precipitation was
151 concentrated between May and August of each year, with only 17% of the precipitation occurring

152 between January and April, and 21% occurring between September and December. In addition, the
153 highest precipitation occurred in June, whereas the lowest precipitation occurred in December. There is
154 no significant difference in annual precipitation amount among Types I, II and III lithological regions.
155 The significant difference in monthly precipitation amount only exhibited in June, July and August,
156 when the precipitation in Type I lithological regions was significantly higher than those in Types II and
157 III lithological regions ($p < 0.01$).

158

159 **4.3 Relationship between vegetation growth pattern and precipitation in different lithological** 160 **regions**

161 The relationship between vegetation growth patterns and precipitation varied between different
162 lithological regions (Fig. 4). An analysis of the EVIs corresponding to various levels of precipitation
163 showed that in months with precipitation less than 150 mm, the EVIs for Type I lithological regions
164 were significantly higher than those of Types II and III lithological regions (type I -type II: $p < 0.01$;);
165 in months with precipitation greater than 150 mm but less than 250 mm, significant differences were
166 not observed in the EVIs among the three types of lithological regions; and in months with a
167 precipitation greater than 250 mm, the EVIs for Type I lithological regions were again higher than
168 those for Types II and III.

169

170 **5. Discussion**

171 The analysis of the relationship between vegetation growth patterns and precipitation in regions
172 with different types of bedrock shows that the properties of bedrock alter the relationship between
173 vegetation and precipitation. In regions where the bedrock contains relatively high amounts of Ca,
174 vegetation growth is more sensitive to drought stress. The insignificant difference in vegetation growth
175 among regions with different lithologies during periods with high precipitation demonstrates that there
176 is a threshold of precipitation amount for the mediation of bedrock on the precipitation-determined
177 vegetation growth.

178 The solubility of bedrock is related to its composition. Because the dissolution of carbonate rocks
179 is caused by the hydrolysis of calcium carbonate (CaCO_3) (Ford and Williams, 2011; Estrada-Medina et
180 al., 2013), rocks with higher carbonate content, including both calcite (CaCO_3) and dolomite
181 ($\text{CaMg}(\text{CO}_3)_2$) present higher dissolution rates. Laboratory simulations have shown that the dissolution

182 rates of carbonates are several tens to hundreds of thousands of times those of silicates (Dreybrodt,
183 1990). Due to their high solubility (Bakalowicz, 2005; Zhang et al., 2012), carbonate rocks develop
184 large numbers of cracks on their surface as a result of precipitation-induced water erosion, which
185 significantly increases the infiltration of water, and therefore, limits the growth of aboveground
186 vegetation through prolonged drought period (Liu et al., 2019). As a result, the regions where the
187 bedrock with high Ca content commonly exhibit low water storage capacity (Karasuyama et al., 2011).
188 Therefore, under low precipitation period, vegetation growth could be limited by drought stress. In
189 contrary, water storage of regolith can help vegetation to resist drought in a region with low Ca
190 concentration bedrock.

191 It is noteworthy that under high precipitation condition, the vegetation growth in Type I bedrock
192 regions was significantly superior to those in Types II and III regions, which might be due to the
193 regolith layer in regions with carbonate rocks has low water storage capacity. In addition, vegetation
194 coverage in these regions is low. As a result, precipitation can easily cause floods or mudflows, thereby
195 affecting vegetation growth (Xu et al., 2008). Another possibility is that vegetation in regions with
196 carbonate rocks has low tolerance to floods (Rong and Xiong, 2007). Because regions with carbonate
197 rocks are prone to droughts, a number of types of vegetation have developed an aerial root structure
198 (Liu et al., 2011). Heavy precipitation renders the root systems of these types of vegetation unable to
199 respire normally, thereby damaging or destroying them and consequently affecting vegetation growth.
200 This finding reflects the vulnerability of ecosystems in regions with carbonate rocks. Due to severe soil
201 erosion, vegetation in regions with carbonate rocks is more easily affected by extreme weather
202 conditions than in other regions.

203 We do not intend to deny that bedrock can affect vegetation growth in a number of other ways.
204 For example, the soil composition strongly relies on bedrock (Xiang et al., 2011). Some important
205 nutrient elements (e.g., phosphorus, iron, and magnesium) are mainly originated from the weathering
206 of rocks. In addition, the physical and chemical properties of soil are affected by bedrock. For example,
207 the clay component of a soil primarily comes from the weathering of silicon and magnesium
208 compounds in rocks (Williamson et al., 2004). However, the availability of soil nutrients is greatly
209 associated with available water in the soil, and the percentage of clay component also contributes to
210 soil water availability.

211

212 **5. Conclusions**

213 In this study, the determination and classification of changes in the chemical elements in stream
214 sediments shows that these changes reflect the difference in bedrock very well and suggests that stream
215 sediments can be used as a basis for distinguishing bedrock types, which could provide a useful tool for
216 studying the mediation of bedrock on vegetation growth on a large scale. The effects of bedrock are
217 found to be significant in karst regions, even on a regional scale (approximately 170,000 km²), based
218 on remote sensing images and stream sediment data. The bedrock-mediated available water can
219 regulate the relationship between precipitation and vegetation growth on a large scale. There is a
220 threshold of less than 150 mm monthly precipitation amount for limiting vegetation growth in the karst
221 landscape in the subtropical region of China. As regions with carbonate bedrock cover 15% of the
222 Earth's surface, this kind of threshold should be taken into account when studying responses of
223 vegetation growth to climate change in the karst landscape.

224

225 **Acknowledgements**

226 We would like to express our sincere gratitude to Lu Zhang for his guidance in the preparation of
227 this article and Jie Liu for her help in the preparation of the figures. This study was financially
228 supported by the Karst Critical Zone Project under grant No. 415711130044.

229

230 **References**

- 231 Albanese, S., Vivo, B.D., Lima, A., Cicchella, D., 2007. Geochemical background and baseline values
232 of toxic elements in stream sediments of Campania region (Italy). *J. Geochem. Explor*, 93(1),
233 21-34.
- 234 Bakalowicz, M., 2005. Karst groundwater: a challenge for new resources. *Hydrogeol. J.*, 13(1),
235 148-160.
- 236 Buermann, W., 2014. Vegetation productivity patterns at high northern latitudes: a multi-sensor satellite
237 data assessment. *Global. Change. Biol*, 20(10), 3147-3158.
- 238 Chapman S.C., 2015. The shifting influence of drought and heat stress for crops in Northeast Australia.
239 *Global. Change. Biol*, 21(11), 4115-4127.
- 240 Cheng, Q., Agterberg, F.P., 2009. *Singularity analysis of ore-mineral and toxic trace elements in stream*
241 *sediments*. Pergamon Press, Inc.

242 Cressie, N.A.C., Whitford, H.J., 2010. How to Use the Two Sample t-Test. *Biometr. J.*, 28(2), 131-148.

243 De Jong, R., Schaepman, M.E., Furrer, R., De Bruin, S., Verburg, P.H., 2013. Spatial relationship
244 between climatologies and changes in global vegetation activity. *Global. Change. Biol.*, 19(6),
245 1953-1964.

246 De Jong, R., Verbesselt, J., Schaepman, M.E., De Bruin, S., 2012. Trend changes in global greening
247 and browning: contribution of short-term trends to longer-term change. *Global. Change. Biol.*,
248 18(2), 642-655.

249 Dreybrodt, W., 1990. The Role of Dissolution Kinetics in the Development of Karst Aquifers in
250 Limestone: A Model Simulation of Karst Evolution. *J. Geol.*, 98(5), 639-655.

251 Estrada-Medina, H., Graham, R.C., Allen, M.F., Jiménez-Osornio, J.J., Robles-Casolco, S., 2013. The
252 importance of limestone bedrock and dissolution karst features on tree root distribution in northern
253 Yucatán, México. *Plant. Soil.*, 362(1-2), 37-50.

254 Feng, Q., 2009. *Geochemical Atlas of Guizhou Province*. Geological Publishing House, Beijing.

255 Ford, D., Williams, P.W., 2011. Karst Geomorphology and Hydrology. *Geograph. J.*, 157(1), 87.

256 Fridley, J.D., Grime, J.P., Askew, A.P., Moser, B., Stevens, C.J., 2011. Soil heterogeneity buffers
257 community response to climate change in species - rich grassland. *Global. Change. Biol.*, 17(5),
258 2002-2011.

259 Garbulsky, M.F., Penuelas, J., Papale, D., Filella, I., 2008. Remote estimation of carbon dioxide uptake
260 by a Mediterranean forest. *Global. Change. Biol.*, 14(12), 2860-2867.

261 Guay, K.C., Beck, P.S.A., Berner, L.T., Goetz, S.J., Baccini, A., Jolly, W.M., Running, S.W., 2004.
262 Effects of precipitation and soil water potential on drought deciduous phenology in the Kalahari.
263 *Global. Change. Biol.*, 10(3), 303-308.

264 Hahm, W.J., Riebel, C.S., Lukens, C.E., Araki, S., 2014. Bedrock composition regulates mountain
265 ecosystems and landscape evolution. *PNAS*, 111: 3338-3343.

266 Kirkwood, C., Everett, P., Ferreira, A., Lister, B., 2016. Stream sediment geochemistry as a tool for
267 enhancing geological understanding: An overview of new data from south west England. *J.*
268 *Geochem. Explor.*, 163, 28-40.

269 Liu, C., Liu, Y., Guo, K., 2011. Ecophysiological adaptations to drought stress of seedlings of four
270 plant species with different growth forms in karst habitats. *Chin. J. Plant. Ecology*, 35, 1070-1082.
271 (in Chinese with English abstract)

272 Liu, H., Jiang, Z., Dai, J., Wu, X., Peng, J., Wang, H., Meersmans, J., Green, S.M., Quine, T.A., 2019.
273 Rock crevices determine wood and herbaceous plant cover in the karst critical zone. China. Earth.
274 Sci., doi:10.1007/s11430-018-9328-3.

275 Lobell, D.B, Hammer G.L., Chenu, K., Zheng, B., McLean, G., Medlyn, B.E., De Kauwe, M.G.,
276 Zaehle, S., Walker, A.P., Duursma, R.A., Luus, K., Ellsworth, D.S., 2016. Using models to guide
277 field experiments: a priori predictions for the CO₂ response of a nutrient- and water-limited native
278 Eucalypt woodland. Global. Change. Biol, 22(8), 2834-2851.

279 Morford, S.L., Houlton, B.Z., Dahlgren, R.A., 2011. Increased forest ecosystem carbon and nitrogen
280 storage from nitrogen rich bedrock. Nature, 477(7362), 78-81.

281 Mori, U., Mendiburu, A., Lozano, J.A., 2016. Distance Measures for Time Series in R: the TSdist
282 Package. NATO. Sci, 8(2), 159-171.

283 Neff, J.C., Reynolds, R., Sanford, R.L., Fernandez, D., Lamothe, P., 2006. Controls of bedrock
284 geochemistry on soil and plant nutrients in southeastern Utah. Ecosystems, 9(6), 879-893.

285 Rong, L., Xiong, K., 2007. Drought-resistance characters of karst plant adaptability in Huajiang karst
286 gorge I: Root system of *Zanthoxylum planispinum* var. *dintanensis* and its soil environment. J.
287 Guizhou. Normal. University (Natural Sciences). 25(4): 1-7. (in Chinese with English abstract)

288 Serrà, J., Arcos, J.L., 2014. An empirical evaluation of similarity measures for time series classification.
289 Knowl-Based. Sys, 67(3), 305-314.

290 Sun, C., Wang, S., Zhou, D., Li, R., Li, Y., 2002. Differential weathering and pedogenetic
291 characteristics of carbonate rocks and their effect on the development of rock desertification in
292 karst regions. Acta Mineralogica Sinica, 22(4), 308-314. (in Chinese with English abstract)

293 Vital, H., Statterger, K., 2000. Major and trace elements of stream sediments from the lowermost
294 Amazon River. Chem. Geol, 168(1), 151-168.

295 Wang, B., Yang, S., Lü, C., Zhang, J., Wang, Y., 2010. Comparison of net primary productivity in karst
296 and non-karst areas: a case study in Guizhou Province, China. Environ. Earth. Sci, 59(6):
297 1337-1347.

298 Wang, S.J., Liu, Q.M., Zhang, D.F., 2004. Karst rocky desertification in southwestern China:
299 Geomorphology, landuse, impact and rehabilitation. Land. Degrad. Dev, 15(2), 115-121.

300 Williamson, T.N., Graham, R.C., Shouse, P.J., 2004. Effects of a chaparral-to-grass conversion on soil
301 physical and hydrologic properties after four decades. Geoderma 123(1-2): 99-114.

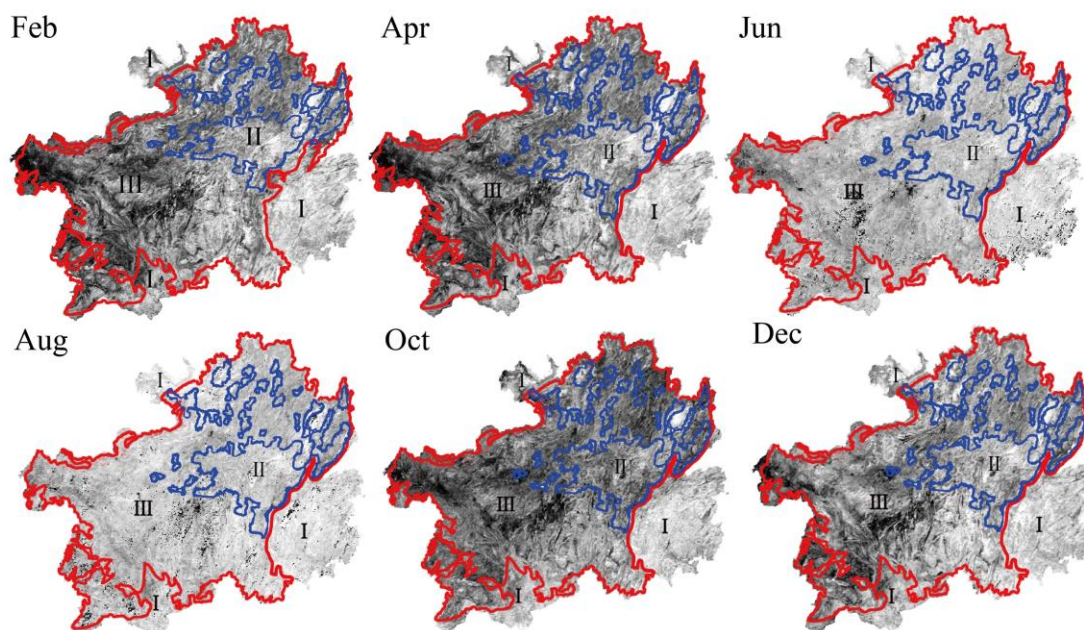
302 Xu, Y., Shen, S., Chen, L., 2008. Geological Disasters and Mitigation Measures along the Coastal
303 Cities of China: Springer Berlin Heidelberg.

304 Yang, J., Nie, Y., Chen, H., Wang, S., Wang, K., 2016. Hydraulic properties of karst fractures filled
305 with soils and regolith materials: Implication for their ecohydrological functions. *Geoderma*, 276,
306 93-101.

307 Zhang, Q., Liu, Z., Luo, J., Bai, X., Ye, Z., 2012. A study of the effects of lithology on landform
308 evolution of Shibing Karst World Natural Heritage Nominated Site in Guizhou Province. *J.*
309 *Southwest University (Natural Science Edition)*, 34(6): 114-120. (in Chinese with English
310 abstract)

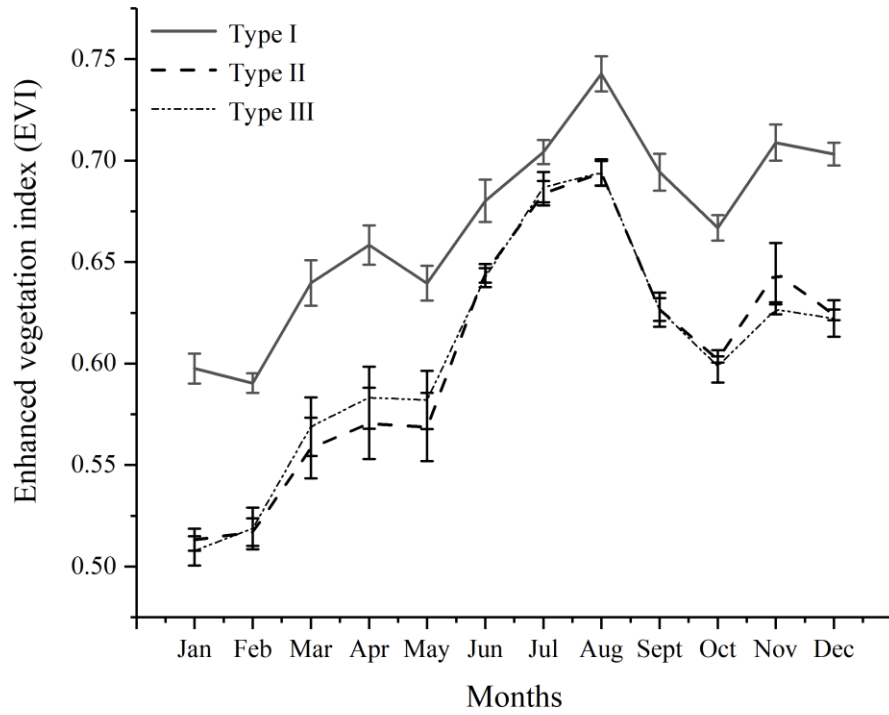
311

312 **Fig. 1 Division of lithological regions based on stream sediment and their temporal changes in the**
313 **EVI.** Within the red borders are Type III bedrock regions, where the bedrock has relatively high Ca
314 content (consists mainly of limestone and dolomite) and karst landforms are well developed; within the
315 blue borders are Type II bedrock regions, where the main bedrock types are dolomite and
316 sandstone-shale; the remaining area is Type I bedrock, where the main bedrock types are clastic and
317 igneous rocks. The grey levels from black to white represent EVI from 0 to 1.



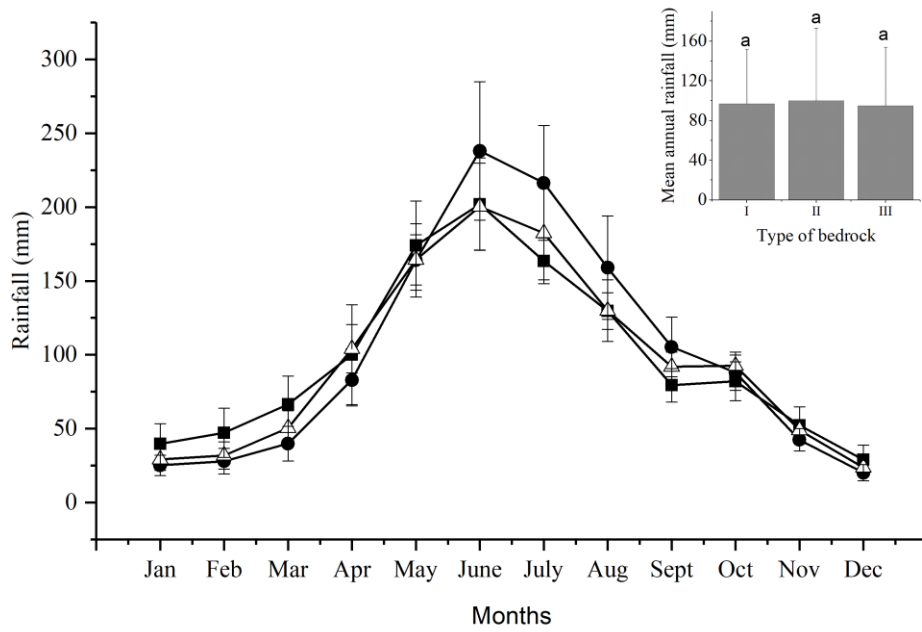
318
319
320
321
322
323
324
325
326
327
328
329
330

331 **Fig.2 Vegetation growth patterns in different lithological regions of Guizhou Province.** The curves
332 show the changes in the EVI for different lithological regions, with the curves of different types
333 representing the different lithological regions.



334
335
336
337

338 **Fig.3 Temporal distribution of precipitation in different lithological regions.** The dots show
339 precipitation conditions in Type I lithological regions; the triangles show precipitation conditions in
340 Type II lithological regions; the squares show precipitation conditions in the Type III lithological
341 regions. The histogram in the upper right corner shows the difference in annual precipitation between
342 lithological regions.

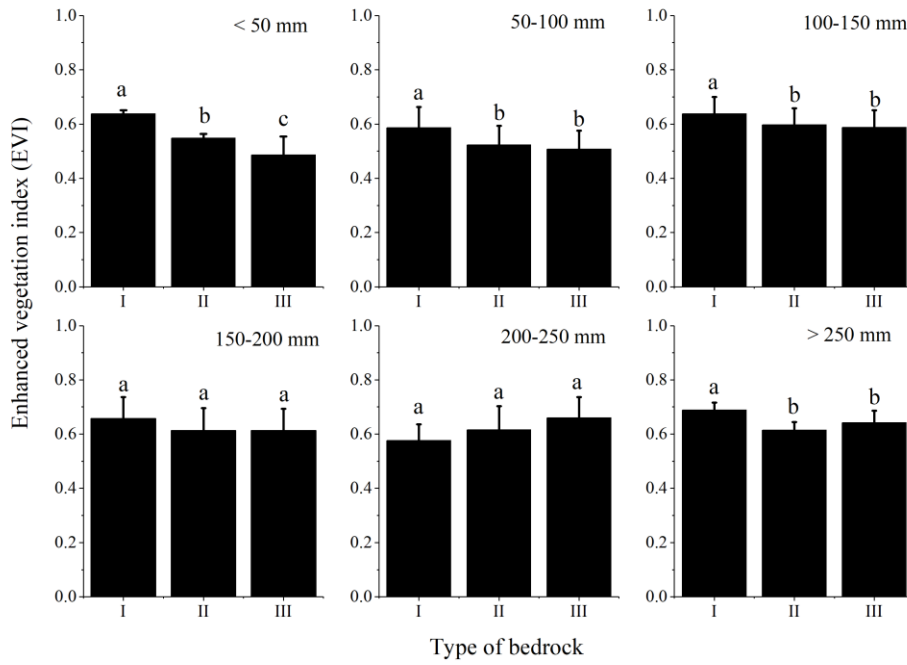


343
344
345
346
347
348
349
350
351
352
353
354
355
356
357
358
359

360

361 **Fig. 4 Relation between bedrock type and vegetation growth (EVI) under various precipitation**

362 **conditions.** The value at the upper right corner of each histogram is the monthly precipitation.



363

364

365

366